

EQUIVALENT WIDTHS OF ATOMIC LINES IN SUNSPOT SPECTRA

K. D. ABHYANKAR AND A. S. RAMANATHAN

Kodaikanal Observatory, India

Received September 30, 1954

ABSTRACT

Equivalent widths of 82 $Cr\ I$ lines, 70 $Fe\ I$ lines, and 74 $Ti\ I$ lines are measured in the spectra of four sunspots of average area 55 millionths of the visible hemisphere of the sun. Separate curves of growth for $Cr\ I$, $Fe\ I$, and $Ti\ I$ are constructed. Excitation temperatures of $4030^\circ \pm 80^\circ$, $4200^\circ \pm 150^\circ$, and $3800^\circ \pm 100^\circ$ are obtained for $Cr\ I$, $Fe\ I$, and $Ti\ I$, respectively.

I. INTRODUCTION

Physical conditions in a stellar object are derived generally from a study of its continuous spectrum and its absorption- or emission-line spectrum. Both aspects of the solar spectrum have been observed in considerable detail, and the observations have been used by many investigators for constructing a satisfactory solar model. In the case of sunspots, however, the observational data are mainly confined to the continuous spectrum of sunspots, as in the works of Pettit and Nicholson (1930), Wanders (1935), Wormell (1936), Richardson (1933), Waldmeier (1939), and the more recent works of Das and Ramanathan (1953), Michard (1953), and Ramanathan (1954). But, except for the semiquantitative but extensive study of atomic lines in the sunspot spectrum by Charlotte Moore (1932) and the measurement of equivalent widths of about 50 $Fe\ I$ and $Ti\ I$ lines by ten Bruggencate and von Klüber (1939), there is a complete lack of quantitative observational material on the Fraunhofer spectrum of sunspots. One object of the present study is to provide sufficiently accurate quantitative data with respect to some absorption lines in the spectrum of sunspots. In this paper are reported the measurements of equivalent widths of 82 $Cr\ I$ lines, 70 $Fe\ I$ lines, and 74 $Ti\ I$ lines.

C. Moore (1932) has estimated the intensities of 6312 atomic lines in the spot spectrum on the Rowland scale of intensities. By comparing the intensities of 1000 lines of Ca , Ti , Cr , Mn , Fe , and Ni in the spectra of the spot and the photosphere, she derived a value of $\Delta\theta = -0.19$, where $\theta = 5040/T$. Further, by assuming an effective temperature of 5740° for the photosphere, she derived an effective temperature of 4720° for the spot. But if we bear in mind that the temperatures concerned here are not effective temperatures but excitation temperatures and that the excitation temperature of the photosphere is much lower than 5740° , the value for the spot needs modification. In fact, ten Bruggencate and von Klüber (1939) have obtained a much lower value of 3800° for the excitation temperature of sunspots from the lines of $Fe\ I$ and $Ti\ I$. This point will be discussed in detail later in this paper. But in order to provide stronger observational support for this argument, in the latter part of this paper the excitation temperature for sunspots is redetermined by constructing separate curves of growth for the lines of $Cr\ I$, $Fe\ I$, and $Ti\ I$.

II. OBSERVATIONAL MATERIAL

a) GENERAL

The spot spectrum plates used in this investigation are the same as those taken by one of the authors (Ramanathan 1954) with the plane-grating spectrograph of the Kodaikanal Observatory, and used by him for measuring the flux ratio I_S/I_P of umbral to photospheric intensity throughout the visible spectral range. The optical arrangement, photographing technique, and method of standardizing the plates are all fully described

in his papers. Here only the procedure of making the microphotometer records will be described. But the information about the observed spots is retabulated in Table 1 for ready reference.

TABLE 1
KKL NUMBERS AND AREAS OF THE OBSERVED SUNSPOTS

Spot No.	Dates of Observations	Date of Central Meridian Passage	Area of Spot in Millionths of Visible Hemisphere	Area of Umbra in Millionths of Visible Hemisphere
KKL 9920.....	Dec. 18, 19, 20, 1952	Dec. 18, 1952	470	85
KKL 9922.....	Dec. 20, 22, 23, 1952	Dec. 20, 1952	285	50
KKL 9929.....	Jan. 10, 11, 12, 1953	Jan. 12, 1953	175	29
KKL 9930.....	Jan. 14, 15, 1953	Jan. 15, 1953	177	40

b) MICROPHOTOMETER RECORDS

Two plates of proper densities for each of the two larger spots (KKL 9920 and KKL 9922) and one plate for each of two smaller ones (KKL 9929 and KKL 9930) were selected in every one of the five spectral regions, viz., *Na D* region, *Mg b* region, *H β* region, *Ca g* region, and *H* and *K* region. These plates were run through the Cambridge recording microphotometer of this observatory. The plate to be measured was placed with the direction of dispersion parallel to the direction of motion of the plate. To insure exact parallelism, the scanning spot of light was first brought to one end of the spectrum and was adjusted to be on the central portion of the umbra by getting the maximum deflection of the electrometer needle. The plate was then moved so that the other end of the spectrum was brought under the scanning spot of light. If the direction of dispersion was not parallel to the direction of motion, the spot of light did not fall on the center of the umbra, and the deflection was not maximum. In that case the plate was rotated around a vertical axis by means of the screw provided for this purpose and was also moved crosswise until the deflection was maximum. The plate was then run backward to the original position, and the adjustment was made again to get maximum deflection. The process was repeated until the spot of light remained over the umbral region of the spot spectrum throughout the run of the plate. If the records were now made by setting the scanning spot of light on the middle of the umbra to start with, only the spectrum of the umbra would be recorded. Each microphotometer tracing covered a range of about 14 Å (1 cm of the plate) with a magnification of 50 on the recording paper. In this way a dispersion of 1.435 Å/mm on the plate was magnified to 0.287 Å/cm on the record. About 25 records were thus necessary to cover the complete range of 300 Å on the plate. The scanning slit of the microphotometer had a width of 0.03 mm, while the slit of the spectrograph was 0.04 mm wide, so that the resolving power of the spectrograph was not affected by that of the scanning slit of the microphotometer. The length of the scanning slit was always kept less than the diameter of the umbra of the spot under examination. Thus if the scanning slit is properly adjusted on the center of the umbra, only the unmixed spectrum of the spot umbra would be analyzed.

For each plate four microphotometer tracings of the standardization spectrum also were made at equal wave-length intervals, and each record was used for about 75 Å to convert densities into intensities.

c) REDUCTION OF OBSERVATIONS

Eighty-two lines of *C τ I*, 70 lines of *Fe I*, and 74 lines of *Ti I*, chosen according to their membership in multiplets and according to the availability of theoretical or experimental

gf-values, were identified by comparing the microphotometer records with those in the *Utrecht Photometric Atlas* of the solar spectrum. In this comparison the intensities of the lines in photospheric and spot spectra, on the Rowland scale, as given in the Mount Wilson *Revised Rowland Table*, were used. There was not much difficulty in identification, though on some records a few lines could not be definitely identified because of too much blending with other lines or because of their faintness. These doubtful cases were ignored. However, in many cases the line wings had to be drawn plausibly, to reach the continuum. This cannot be avoided in the case of the spot spectrum, which is extremely complicated, and hence not all the lines have clear-cut wings reaching the continuum.

The density profile of every identified line was converted into an intensity profile by means of the standardization-curves in the usual way. The value of r , the ratio of the intensity at a point in the line to the intensity at the corresponding point in the continuum, was determined. In most of the lines, except for a few broad ones, the continuum intensity was constant in the region of the line. Equivalent width was then easily

TABLE 2
PROBABLE ERRORS OF MEAN EQUIVALENT WIDTHS

Assigned Weight	No. of Individual Measures	Per Cent Probable Error of Mean	Assigned Weight	No. of Individual Measures	Per Cent Probable Error of Mean
4.....	{ 6	6	2.....	3 and 4	12
	{ 5	4			15
3.....	{ 6	10	1.....	{ 2
	{ 5	8			
	{ 4	6			

obtained by working out the area $\int(1-r)d\lambda$ by the trapezoidal rule. On an average, four to six individual measurements were possible for every line. The average equivalent widths of the lines in milliangstroms are tabulated in the fourth column of Tables 3, 4a and 4b, and 5. These tables include, also, the estimated intensities of the lines in the spot spectrum in the ninth column (from the *Revised Rowland* table) and the weight assigned to every line in the eighth column. In assigning the weights, both the number of individual measurements and the probable error of the mean were taken into consideration. Table 2 gives the criteria used.

III. SOURCES OF ERROR AND ACCURACY OF MEASUREMENTS

The following principal sources of error should be mentioned:

a) *Scattering of photospheric light into the umbral spectrum.*—In the case of measurement of the continuous spectrum of the spot umbra, the amount of light scattered into the umbra can be estimated roughly by Wanders' (1935) method. But it is very difficult and uncertain to get an idea of the effect of scattering in the case of Fraunhofer lines. But from the small scattering corrections for the ratio of umbral to photospheric intensity obtained by Ramanathan (1954), we expect the error on account of scattering to be small. It has been completely neglected in this investigation.

b) *Stray light inside the spectrograph.*—We have not used a monochromator to limit the spectral range admitted into the spectrograph. Instead of that, we have used colored filters to allow only a few hundred angstroms to enter the spectrograph. Stops at suitable places inside the spectrograph further reduced the stray light. The plates also did not show any appreciable background of scattered light. A small amount of scattering

TABLE 3

LINES OF Cr I

Multiplet No.	λ in Å	Est. Int. (RM) in Spot Sp.	Observed V in mÅ	X_{λ} in V	log g^{λ}		Wt.	Remarks
					log W/λ	log V/λ		
1	4254.35	12	314	0.000	-1.252	-4.132	4	
	4274.61	12	279	0.000	-1.355	-4.185	4	
	4289.73	8	359	0.000	-1.499	-4.077	4	
7	5208.43	9	417	0.937	-0.652	-4.097	4	
	5206.05	8	380	0.937	-0.801	-4.137	4	
	5204.52	-	216	0.937	-1.021	-4.322	3	Blend Fe 5204.60
8	5021.93	0	027	0.937	-1.807	-5.269	4	
	5051.91	1	071	0.937	-3.344	-4.892	4	
	5072.92	3	064	0.937	-3.172	-4.899	4	
9	4942.49	4	077	0.937	-2.817	-4.807	4	
	4964.94	3	062	0.937	-2.996	-4.904	4	
18	5409.80	9	257	1.026	-1.359	-4.323	3	
	5345.81	10	176	0.999	-1.634	-4.483	3	
	5296.70	8	114	0.979	-2.029	-4.667	3	
	5344.33	9	152	0.999	-1.813	-4.545	3	
	5298.29	7	231	0.979	-1.819	-4.560	3	
	5300.76	6	362	0.979	-2.709	-4.932	3	
	5285.73	3	175	0.964	-2.372	-4.479	4	Cr - Ni (Weak)
	5247.98	4	168	0.997	-2.259	-4.495	3	
20	5068.31	1	019	0.999	-3.548	-5.426	3	Cr - Ti
	5123.47	0	033	1.026	-3.349	-5.191	1	
	5091.89	1	031	0.999	-3.600	-5.216	4	
22	4344.51	6	107	0.999	-1.316	-4.609	4	
	4339.46	6	182	0.979	-1.404	-4.485	4	
	4337.57	4	119	0.964	-1.687	-4.566	4	
	4339.72	4	155	0.997	-1.922	-4.447	4	
	4364.99	4	166	1.026	-1.915	-4.418	4	
	4371.29	4	123	0.999	-1.438	-4.531	4	
	4359.63	5	142	0.979	-1.776	-4.487	4	Blend Cr 4359.50
	4351.06	5	082	0.964	-1.921	-4.725	4	
	4412.26	2	031	1.026	-2.736	-5.153	4	
	4391.77	4	102	0.999	-2.593	-4.634	4	Blend Cr + 4391.67 & Co 4391.88
4373.27	3	043	0.979	-2.531	-5.007	4	V - Cr	
30	4895.78	2	058	2.533	-0.857	-4.925	3	
31	4829.37	4	217	2.534	-0.686	-4.347	1	
	4861.85	2	134	2.534	-1.073	-4.560	4	On the wing of H β
	4888.53	3	039	2.533	-1.165	-5.098	2	Blend Fe 4888.64
	4903.26	7	093	2.531	-1.106	-4.722	3	Blend Fe 4903.33
35	4153.81	-	063	2.534	-0.411	-4.819	3	Blend Fe 4153.91
	4191.28	-	021	2.533	-0.639	-5.300	3	Cr - Cr (Weak)
	4203.37	3	033	2.531	-0.810	-5.083	3	Fe - Cr
	4204.20	0	032	2.533	-1.267	-5.119	2	V - Cr?
36	4037.30	-	027	2.534	-0.890	-5.175	3	
59	5222.69	2	043	2.696	-1.373	-5.089	4	
	5239.97	1	027	2.697	-1.122	-5.288	4	
60	5013.31	4	054	2.697	-0.815	-4.968	4	Ti - Cr
	5067.70	1	032	2.697	-1.015	-5.200	3	Blend Co 5067.78
	5144.68	1	052	2.697	-1.335	-4.995	1	Cr - (Co)
64	4295.76	4	062	2.696	-0.176	-4.841	3	
	4340.14	1	153	2.696	-0.492	-4.453	1	Ti - Cr
	4381.12	1	039	2.697	-0.577	-5.051	3	
	4297.05	2	158	2.697	-0.781	-4.435	4	Blend Cr 4295.96
84	4343.21	4	087	2.698	-0.931	-4.698	3	Blend Fe 4343.27
	4387.40	0	031	2.970	-0.690	-5.151	3	Cr ?
94	5328.33	3	295	2.901	+0.225	-4.297	4	
	5297.39	4	145	2.897	+0.099	-4.563	3	
	5329.15	5	126	2.921	-0.096	-4.626	4	
	5298.03	2	106	2.897	-0.015	-4.699	3	
	5275.76	2	098	2.877	-0.133	-4.731	3	
96	5329.60	1	043	2.921	-0.622	-5.093	4	
	5276.07	3	144	2.877	-0.291	-4.564	3	
	4261.35	1	115	2.901	-0.267	-4.569	3	
103	4272.90	2	058	2.897	-0.490	-4.867	4	
	4327.90	1	064	2.990	-0.304	-4.836	3	Cr - Cr
104	4375.34	1	065	2.970	-0.245	-4.828	4	
	4363.11	2	062	2.950	-0.212	-4.847	4	Cr - Cr
104	4374.18	1	073	2.990	+0.061	-4.778	4	
	4346.83	1	043	2.970	-0.163	-5.005	4	
105	4255.51	1	061	2.990	-0.223	-4.844	4	Cr - Fe
	4240.70	1	069	2.970	-0.330	-4.789	3	
128	4403.38	1	056	3.000	-0.568	-4.896	3	Cr + Cr
	4423.27	1	062	3.000	-0.461	-4.893	3	Cr ?
132	4216.36	0	039	3.001	-0.278	-5.034	2	
	4222.73	0	031	3.000	-0.317	-5.134	3	
143	4022.27	4	070	3.099	+0.237	-4.847	4	
	4287.01	2	056	3.070	+0.083	-4.941	3	Cr - Ni
	4270.22	2	073	3.070	+0.018	-4.824	3	Cr - Ni
166	4954.81	3	060	3.110	-0.148	-4.917	3	
	4956.34	2	048	3.100	-0.148	-5.012	4	
207	5196.45	1	078	3.430	+0.140	-4.824	4	
	5255.13	0	096	3.449	+0.107	-4.738	1	
225	5340.46	1	040	3.423	-0.365	-5.125	3	

TABLE 1 (a)

Multiplet No.	λ in Å	Est. Int. (RR) in Spot Sp.	Observed		log SRI λ		Wt.
			W in mÅ	χ_e in V	log \bar{E}/λ_e	log W/ λ	
318	4890.77	6	231	2.863	+6.283	-4.326	3
	4891.50	8	451	2.839	+6.463	-4.035	3
	4903.33	7	187	2.870	+5.782	-4.523	3
	4919.00	7	315	2.853	+6.291	-4.194	3
	4920.52	10	456	2.820	+6.691	-4.033	4
	4938.82	6	142	2.863	+5.649	-4.541	4
	4985.56	5	100	2.853	+5.446	-4.698	4
	5006.12	7	276	2.820	+6.084	-4.259	4
	5044.22	4	074	2.839	+5.051	-4.834	4
	383	5068.77	7	110	2.927	+5.319	-4.664
5192.36		6	282	2.985	+6.170	-4.265	4
5232.95		9	359	2.927	+6.567	-4.164	4
5266.57		8	347	2.985	+6.284	-4.181	4
5281.80		9	156	3.025	+5.833	-4.530	3
553	5215.39	4	118	3.252	+5.988	-4.645	3
	5217.40	4	109	3.197	+5.928	-4.680	4
	5229.86	4	112	3.269	+5.747	-4.669	4
	5253.47	3	074	3.269	+5.145	-4.851	4
	5263.32	4	119	3.252	+5.845	-4.646	4
	5273.17	3	104	3.278	+5.754	-4.705	3
	5283.63	10	210	3.227	+6.293	-4.401	3
	5302.31	7	141	3.269	+5.992	-4.575	3
	5324.19	8	330	3.197	+6.630	-4.208	3
	5339.04	6	149	3.252	+6.049	-4.554	4
5393.18	7	168	3.227	+5.935	-4.507	4	
965	5001.87	6	100	3.865	+6.694	-4.699	3
	5014.95	2	131	3.926	+6.533	-4.583	4
	5022.24	2	101	3.967	+6.363	-4.697	4
984	4973.11	6	054	3.940	+6.097	-4.891	3
	4985.26	3	057	3.912	+6.286	-4.982	3
	5005.72	4	105	3.867	+6.534	-4.678	4
	5048.44	2	056	3.943	+5.631	-4.955	4

TABLE 1 (b)

Multiplet No.	λ in Å	Est. Int. (RR) in Spot Sp.	Observed V in mÅ	log SRI λ			Wt.	Remarks
				χ_e in V	log \bar{E}/λ_e	log W/ λ		
1	5110.41	9	116	0.000	-4.369	-4.644	3	
	5156.29	5	105	0.000	-4.705	-4.692	3	
	5168.91	5	251	0.051	-4.525	-4.314	4	
	5204.60	12	312	0.087	-4.835	-4.222	4	Blend Cr 5204.51
2	4347.24	2	032	0.000	-4.892	-5.133	4	
	4375.95	9	135	0.000	-3.609	-4.511	4	
	4389.26	3	045	0.051	-4.873	-4.989	4	
	4427.32	9	161	0.051	-3.619	-4.439	4	
	4435.16	4	137	0.087	-4.873	-4.510	3	
4461.66	7	162	0.087	-3.790	-4.440	2		
3	4206.70	6	069	0.051	-4.472	-4.795	4	
	4216.19	5	174	0.000	-3.920	-4.384	4	
	4258.33	4	156	0.087	-4.672	-4.436	4	
	4291.48	3	116	0.051	-4.599	-4.568	4	
15	5269.55	11	515	0.855	-2.018	-4.010	4	
	5328.05	11	424	0.911	-2.169	-4.099	4	
	5371.90	14	431	0.984	-2.345	-4.096	4	
	5397.14	14	330	0.911	-2.635	-4.214	4	
	5405.79	11	391	0.986	-2.489	-4.141	4	
	5429.71	14	415	0.954	-2.541	-4.117	2	
5434.54	8	197	1.007	-2.716	-4.441	1		
36	5171.61	8	207	1.478	-3.207	-4.398	4	
37	5227.19	6	456	1.551	-1.868	-4.059	4	
	5270.39	9	391	1.601	-1.993	-4.130	4	
41	4294.15	9	238	1.478	-1.672	-4.256	3	
	4337.06	7	149	1.551	-2.139	-4.464	3	
	4383.56	15	942	1.478	-0.490	-3.668	4	
	4404.76	10	592	1.551	-0.776	-3.872	4	
	4415.14	8	326	1.601	-1.253	-4.132	4	
42	4202.04	9	342	1.478	-1.301	-4.089	4	
	4290.80	9	333	1.551	-1.308	-4.166	3	
	4271.78	12	741	1.478	-0.842	-3.761	4	
	4307.91	7	828	1.551	-0.733	-3.716	3	
	4325.78	8	619	1.601	-0.673	-3.844	4	Blend Ti+ and Cr both weak.
43	4005.26	6	905	1.551	-1.163	-3.899	4	
	4045.83	28	1066	1.478	-0.466	-3.579	4	
	4063.61	15	873	1.551	-0.611	-3.761	4	
	4071.75	15	601	1.601	-0.666	-3.825	2	

TABLE 5

LINES OF Ti I

Multiplet No.	λ in Å	Est. Int. (RR) in Spot Sp.	Observed V in mÅ	Log $g^{\circ} \lambda$			Wt.	Remarks
				X_e in V	$\log \bar{N}/k$	$\log W/\lambda$		
3	5396.58	3	073	0.000	-4.154	-4.869	4	
	5426.26	4	029	0.020	-3.641	-5.272	3	
4	5147.48*	4	060	0.000	-3.082	-4.933	3	
	5152.19*	3	139	0.020	-3.091	-4.569	4	
	5173.75	4	237	0.000	-2.119	-4.339	4	
	5192.98	5	171	0.020	-1.994	-4.483	4	
	5210.39	6	157	0.048	-1.869	-4.521	3	
	5219.71*	3	050	0.020	-3.363	-5.019	4	
5252.11	1	086	0.048	-3.568	-4.786	4		
5	4997.10*	3	060	0.000	-3.172	-4.921	4	
	5009.65*	4	037	0.020	-3.302	-5.132	4	
	5014.19	-	114	0.000	-2.278	-4.643	4	
	5064.66*	7	082	0.048	-1.909	-4.791	4	Blend 5014.282 & 5014.128
5039.97	5	083	0.020	-2.089	-4.783	4		
11	3982.49	3	127	0.000	-2.349	-4.496	4	
	4009.66	4	121	0.020	-2.737	-4.520	3	Blend Fe 4009.72
12	3981.78	4	163	0.000	-1.354	-4.388	3	Ti - Fe ?
	3989.77	5	129	0.020	-1.283	-4.522	4	
	3998.65	4	215	0.048	-1.011	-4.270	4	
	4008.94	4	083	0.020	-2.063	-4.684	3	Blend Fe 4008.88
4024.58	4	114	0.048	-2.029	-4.548	3		
35	5366.64	2	038	0.815	-3.206	-5.150	4	
	5399.18	3	026	0.809	-3.289	-5.317	4	
37	5238.57*	2	034	0.845	-2.758	-5.188	4	
	5246.57	0	037	0.832	-3.006	-5.152	4	
	5250.92	0	069	0.822	-3.170	-4.882	4	
38	4981.74*	7	116	0.845	-0.535	-4.633	4	
	4991.07*	5	113	0.832	-0.649	-4.645	4	
	4999.51	6	122	0.822	-0.733	-4.643	4	
	5014.28	8	145	0.809	-1.047	-4.539	4	Ti - Fe (Weak)
	5016.17*	5	053	0.845	-1.588	-4.976	4	
	5020.03*	6	080	0.832	-1.445	-4.798	4	
5022.88	6	115	0.822	-1.480	-4.640	4		
5024.85*	7	055	0.815	-1.638	-4.961	4		
43	4299.65	3	263	0.822	-1.872	-4.214	3	
	4314.81	4	114	0.832	-1.360	-4.578	3	
	4326.36	1	176	0.822	-2.106	-4.391	4	
44	4274.60	3	177	0.815	-2.227	-4.383	3	
	4281.38	2	039	0.809	-2.210	-5.040	4	
	4286.02	4	161	0.822	-1.360	-4.425	4	Blend CH 4286.09
	4287.41	2	053	0.832	-1.360	-4.908	3	
	4289.08	4	133	0.815	-1.274	-4.508	4	
	4290.96	6	117	0.809	-1.445	-4.564	4	Ti - CH
	4295.76	4	062	0.809	-1.383	-4.841	3	Ti - Cr
	4298.68	4	113	0.815	-1.135	-4.580	3	
	4300.58	3	254	0.822	-0.930	-4.229	3	CH - Ti
	4301.11	7	268	0.832	-0.837	-4.206	3	Ti - CH (Weak)
4305.92	8	264	0.845	-0.589	-4.213	3	Blend CH 5306.15	
53	4840.89	6	055	0.896	-1.589	-4.945	3	
71	5280.28	5	031	1.048	-2.765	-5.278	2	
	5918.56	6	059	1.062	-2.542	-5.001	4	
72	5266.46	10	079	1.062	-1.819	-4.871	3	
	5299.31	6	063	1.048	-2.046	-4.972	4	
	5222.13	6	038	1.042	-2.366	-5.193	4	
	5941.77	9	068	1.048	-2.485	-4.942	3	
74	5282.40	3	044	1.048	-2.625	-5.079	3	
	5284.43	2	064	1.042	-2.772	-4.917	2	Fe, Ti ?
	5295.79*	3	040	1.062	-2.416	-5.122	4	
80	4055.04	3	130	1.042	-1.783	-4.494	4	Zr, Ti - Fe
	4060.27	1	030	1.048	-1.677	-5.131	2	
	4064.22	2	332	1.048	-1.848	-4.088	3	
	4065.09	2	096	1.048	-1.783	-4.627	2	Ti, Mn
110	5035.92	7	124	1.454	-0.853	-4.609	4	Blend Ni 5035.98
	5036.47	5	124	1.437	-0.961	-4.609	4	
	5038.41*	4	066	1.424	-1.060	-4.883	4	
154	5953.17	6	051	1.879	-1.199	-5.067	4	
	5965.84	6	044	1.871	-1.240	-5.132	4	
	5978.55	6	038	1.865	-1.311	-5.197	3	
156	5265.97	1	159	1.879	-1.207	-4.520	4	
	5283.44	1	074	1.871	-1.280	-4.854	3	
	5297.24	1	060	1.865	-1.314	-4.946	3	
157	4895.09*	4	071	1.879	-0.720	-4.898	3	
	4899.92*	3	051	1.871	-0.837	-4.983	3	Ti - La ⁺ (Weak)
	4913.62*	4	041	1.865	-0.894	-5.079	4	

might, however, have been present in the spectral regions in the neighborhood of the *H* and *K* lines. The presence of small amounts of scattered light inside the spectrograph would not materially affect the equivalent widths.

c) Finite resolving power of the spectrograph.—The finite resolving power would considerably affect the profile of the spectral line. But it would scarcely affect the equivalent width of the line, particularly with the high dispersion of 1.435 Å/mm used here. As we are concerned only with the total absorption in the line, no correction is necessary on this account.

d) Setting of the scanning slit.—This was done with the greatest possible care. The length of the slit was always kept smaller than the diameter of the umbra. But slight adulteration of the umbral spectrum by the spectrum of the neighboring penumbra might have occurred in the case of the smallest spot, viz., KKL 9929.

To form an idea of the accuracy of the measurements, the percentage probable error of the mean equivalent width was determined for every line. It is given in Table 2. This table shows that there is considerable scatter in the individual measurements of a line. This is due to the nonhomogeneity of the spots observed, the umbral areas of which vary from 30 to 85 millionths of the visible solar hemisphere. Moreover, the inherent difficulties in observing the spot spectrum are also responsible for this discord. But as no systematic variation of equivalent widths with the area of the spot was observed, the values of all the four spots were averaged.

If we further compare the equivalent widths of 32 *Fe I* lines in Table 4a and 17 *Ti I* lines marked with an asterisk in Table 5 observed at Kodaikanal with those obtained by ten Bruggencate and von Klüber (1939), it will be evident that our values are systematically lower than their values by about 30 per cent. This is perhaps to be expected, because the spots observed by them were rather larger (80 millionths of the visible solar hemisphere) than those observed by us (average area 55 millionths of visible solar hemisphere). From the recent thesis by Michard (1953) it seems likely that the larger spots are cooler than the smaller ones; if that is so, the lines due to neutral atoms may be expected to be weaker in smaller spots than in the larger ones.

IV. CONSTRUCTION OF THE CURVE OF GROWTH

a) GENERAL

To construct a curve of growth, we generally plot $\log W/\lambda$ against $\log \eta_f \lambda$, where W is the equivalent width, λ the wave length, and η_f the number of atoms responsible for producing the absorption line. By assuming thermodynamic equilibrium, we get,

$$\log \eta_f \lambda = \log \eta_0 + \log g f \lambda - \theta \chi_e + \log \frac{\bar{k}}{\bar{k}_v} + \Delta \log \eta_0,$$

where

f = Oscillator strength of the line,

g = Statistical weight of the lower level,

$\theta = 5040/T$,

χ_e = Excitation potential of the lower level,

η_0 = Number of atoms in the ground state,

\bar{k} = Mean absorption coefficient,

\bar{k}_v = Continuous absorption coefficient for wave length λ ,

and $\log \bar{k}/\bar{k}_v$ and $\Delta \log \eta_0$ are correction terms. The first corrects for the variation of the continuous absorption coefficient with wave length, while the second converts the

values of $\log \eta_f \lambda$ to a single value of B_0/B_1 . Wrubel (1950) has given the corrections $\Delta \log \eta_0$ for converting all measurements to the same value of $B_0/B_1 = \frac{2}{3}$. If we assume a boundary temperature of 3500° for the spot, B_0/B_1 varies from 0.19 to 0.37 as λ varies from 4000 to 5700 Å. As the lowest value of B_0/B_1 in Wrubel's data is $\frac{1}{3}$, the correction $\Delta \log \eta_0$ could not be determined in the present case. For a boundary temperature of 4000° , B_0/B_1 would vary from 0.22 to 0.42 as λ varies from 4000 to 5700 Å. Even then, the correction $\Delta \log \eta_0$ cannot be determined for all lines. But the correction, being always small, will not affect the shape of the curve of growth or the determination of excitation temperature.

Ten Bruggencate (1947) had determined empirically the correction for variation of continuous absorption coefficient. It is now known that the negative hydrogen ion, which is the principal source of opacity in the photosphere, is also the principal cause of opacity in the spot (Michard 1953). The correction was therefore determined from the mean absorption coefficient computed by Chandrasekhar and Münch (1946) and the con-

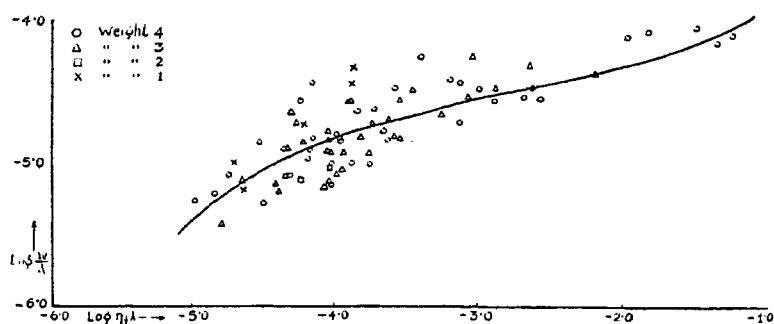


FIG. 1.—Curve of growth for lines of Cr I. $\theta = 1.25$

tinuous absorption coefficient of the negative hydrogen ion given by Chandrasekhar (1946), by assuming an effective temperature of 4200° for the spot.

In the construction of the empirical curve of growth, $\log \eta_0$ need not be taken into consideration, as it forms simply an additive constant. Hence in all cases $\log W/\lambda$ was plotted as ordinate against $\log gf\lambda + \log \bar{k}/k_r - \theta\chi_e$ as abscissa.

b) LINES OF Cr I

The relative gf -values for the lines of Cr I were taken from the experimental data of A. J. Hill and R. B. King (1951). Values of $\log \eta_f \lambda$ for all lines were calculated for various values of θ , and those of $\log W/\lambda$ were plotted against $\log \eta_f \lambda$ in every case. A mean curve of growth was drawn for every value of θ . The deviation Δ from the mean curve was found for all points, and $\Sigma \Delta^2$ was obtained by taking into account the weight assigned to each point. It was found to be least for $\theta = 1.25 \pm 0.025$. This corresponds to an excitation temperature of $4030^\circ \pm 80^\circ$. The curve of growth for Cr I is drawn in Figure 1.

c) LINES OF Fe I

For the lines of Fe I in Table 4b the relative gf -values are available from the data of R. B. King and A. S. King (1938). The excitation temperature was obtained in the case of these lines by the same procedure as was used for Cr I lines. $\Sigma \Delta^2$ was found to be minimum for $\theta = 1.17 \pm 0.015$, corresponding to a temperature of $4300^\circ \pm 50^\circ$.

Experimental gf -values are not available for the Fe I lines in Table 4a. But the theoretical intensities of these lines have been computed by ten Bruggencate and von Klüber

(1939). Values of $\log SRI\lambda$ were obtained from their values of $\log (SRI/\Delta\omega_D)$ by adding $\log 2\pi\sqrt{(2RT/\mu)} = 5.884$, and these values were used in place of $\log gf\lambda$. The rest of the procedure was the same as that used above. In this case the scatter was least for $\theta = 1.23 \pm 0.015$, corresponding to an excitation temperature of $4100^\circ \pm 50^\circ$.

In order to get a single curve of growth, we have adopted a value of 1.20 ± 0.04 for θ , i.e., a value of $4200^\circ \pm 150^\circ$ for the excitation temperature for the lines of $Fe\ I$. Further, the two curves of growth had to be shifted with respect to each other in the direction of the abscissa to make them coincide. The values of $\log SRI\lambda$ had to be reduced by 6.25 to bring them to the same scale as that of $\log gf\lambda$. The composite curve of growth for $Fe\ I$ obtained in this way is drawn in Figure 2.

d) LINES OF $Ti\ I$

The relative gf -values for $Ti\ I$ lines are also given by R. B. King and A. S. King (1938). They were used for drawing a curve of growth for $Ti\ I$ and for getting the excitation tem-

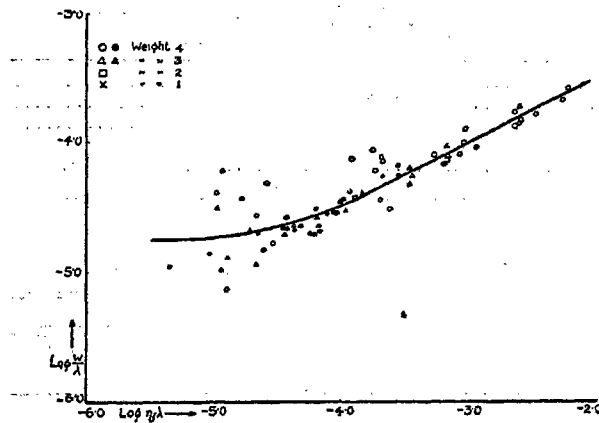


FIG. 2.—Curve of growth for lines of $Fe\ I$. $\theta = 1.20$. For $\circ \triangle \square \times$ points, $\log \eta_f\lambda = \log gf\lambda + \log \bar{k}/k_f - \theta\chi_e$ (lines in Table 4b). For $\bullet \blacktriangle$ points, $\log \eta_f\lambda = \log SRI\lambda + \log \bar{k}/k - \theta\chi_e - 6.25$ (lines in Table 4a).

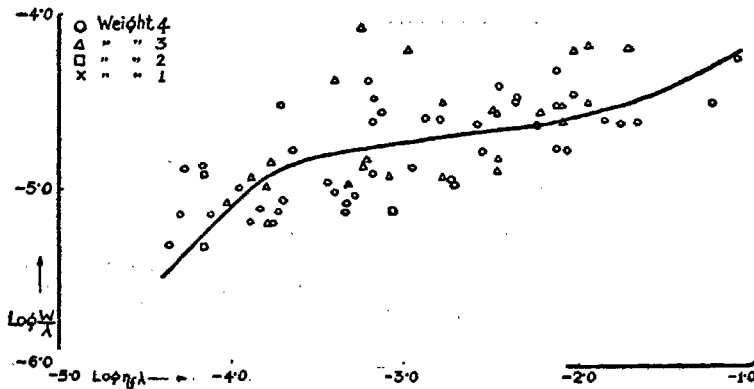


FIG. 3.—Curve of growth for lines of $Ti\ I$. $\theta = 1.325$.

perature for $Ti\ I$. Following the procedure described earlier, we got $\theta = 1.325 \pm 0.04$, i.e., an excitation temperature of $3800^\circ \pm 100^\circ$. The curve of growth for $Ti\ I$ is drawn in Figure 3.

V. DISCUSSION OF THE RESULTS

In order to compare our results with those of others, we have retabulated them in Table 6. From Table 6 it will be seen that the excitation temperatures obtained here are somewhat higher than those obtained by ten Bruggencate and von Klüber (1939). The differences are not great when the errors of measurement are considered. But, as explained in Section III(b), this may be traced back to the smaller area of the spots observed in the present case.

TABLE 6
EXCITATION TEMPERATURE FOR SUNSPOTS

Metal	Present Investigation	ten Bruggencate and von Klüber	C. Moore
$Ti\ I$	$3800^\circ \pm 100^\circ$	3700°
$Fe\ I$	$4200^\circ \pm 150^\circ$	3900°
$Cr\ I$	$4030^\circ \pm 80^\circ$
Ca, Ti, Cr, Mn, Fe, Ni	$4720^\circ \pm 20^\circ$

TABLE 7
EXCITATION TEMPERATURE FOR PHOTOSPHERE

Author	Element	Excitation Temperature for Photosphere
ten Bruggencate and von Klüber (1939)	$\begin{cases} Fe\ I \\ Ti\ I \end{cases}$	5040°
K. O. Wright (1944).....	$\begin{cases} Ti\ I \\ Fe\ I \end{cases}$	$\begin{matrix} 4550^\circ \\ 4900^\circ \end{matrix}$
R. B. King and K. O. Wright (1947)...	$V\ I$	5400°
Sandage and Hill (1950).....	$Cr\ I$	3790°
Michard (1953).....	$\begin{cases} Ti\ I \\ Fe\ I \\ Ti^+ \end{cases}$	$\begin{matrix} 4900^\circ \\ 4670^\circ-5000^\circ \\ 5250^\circ \end{matrix}$

We now return to the question of the high value obtained by Moore (1932). As mentioned in the introduction, we should use the excitation temperature of the photosphere to calculate the excitation temperature of the spot and not the effective temperature. In Table 7 are assembled the values of excitation temperature for the photosphere obtained by various authors.

If we adopt the mean value 4900° for the excitation temperature of the photosphere, we get from Moore's value of $\Delta\theta = -0.19$ a value of 4130 for the excitation temperature of the sunspots. This is in quite good agreement with the values now obtained and also with those by ten Bruggencate and von Klüber.

In conclusion it is our pleasant duty to thank Dr. A. K. Das, director of this Observatory, for his interest and guidance throughout the course of this investigation. We have also to thank Mr. P. Madhavan Mayar for preparing the diagrams for the press.

REFERENCES

- Bruggencate, P. ten. 1947, *Veröff. Göttingen*, No. 76, p. 105.
Bruggencate, P. ten, and Klüber, H. von. 1939, *Zs. f. Ap.*, 18, 284.
Chandrasekhar, S. 1946, *Ap. J.*, 104, 430.
Chandrasekhar, S., and Münch, G., 1946, *Ap. J.*, 104, 446.
Das, A. K., and Ramanathan, A. S. 1953, *Zs. f. Ap.*, 32, 91.
Hill, A. J., and King, R. B. 1951, *J. Opt. Soc. Amer.*, 41, 315.
King, R. B., and King, A. S. 1938, *Ap. J.*, 87, 24.
King, R. B., and Wright, K. O. 1947, *Ap. J.*, 106, 224.
Michard, Raymond. 1953, *Ann. d'ap.*, 16, 217.
Moore, C. E. 1932, *Ap. J.*, 75, 298.
Pettit, E., and Nicholson, S. B. 1930, *Ap. J.*, 71, 153.
Ramanathan, A. S. 1954, *Zs. f. Ap.*, 34, 169.
Richardson, R. S. 1933, *Ap. J.*, 78, 359.
Sandage, A. R., and Hill, A. J. 1951, *Ap. J.*, 113, 525.
Waldmeier, M. 1939, *Astr. Mitt. Zürich*, No. 138, p. 439.
Wanders, A. J. M. 1935, *Zs. f. Ap.*, 10, 15.
Wormell, T. W. 1936, *M.N.*, 96, 736.
Wright, K. O. 1944, *Ap. J.*, 99, 249.
Wrubel, M. 1950, *Ap. J.*, 111, 157.